Geometric analysis and mathematical modelling of spiroid worm

Dr. Illés Dudás[1], Sándor Bodzás[2]

[1]*DSc Professor, Department of Production Engineering, University of Miskolc, H-3515 Miskolc, Egyetemváros, Hungary*
illes.dudas@uni-miskolc.hu
[2]PhD student, *Department of Technical Preparatory and Production Engineering, College of Nyíregyháza, H-4400, Nyíregyháza, Sóstói u. 9-11., Hungary*
bodzassandor@citromail.hu

KEYWORDS : measuring technique, spiroid worm, thread pitch, profile shape error, conicity

Erosion and resharpening of tools, limited punctuality of machine setting, etc. can cause deformation and shape errors of the surfaces. We carried out an up –to-date measuring method that is the measuring of helical surface without circle desk for conical worm. The use of these methods makes it possible to explore the errors arising during production (e.g. thread pitch in axial plane, error of profile shape in axis or remarkable plane etc.) and to define the values of these errors. We worked out the mathematical model of the line forming spiroid worm which is used during the evaluation of measuring results.

Manuscript received: January XX, 2011 / Accepted: January XX, 2011

NOMENCLATURE

- $\vec{r}_{1F}$ - the position vector of the running point of the helical surface;
- h_{mid} - the value of the middle difference;
- h - the value of the differences in the given profile point;
- n - number of the discreet points of the profile;
- f_r. - mistake value.

1. Introduction

The basic problem of the traditional geometrical checking methods is that they treat the two dimensional worm surfaces as a plane figure and consider the planar effects of the different directional dimension errors as cumulative effect (e.g. thread pitch in axial plane, error of profile shape in axis or remarkable plane, etc.) [5]. That is why it is important to give a theoretical basis of appropriate geometrical checking methods, practical usage and application of thread surfaces as three – dimensional figures.

We worked out an up –to-date measuring method using a DEA type 3D measuring machine which can be found in the Laboratory of the Department of Production Engineering of Miskolc University which measures thread surfaces without circle desk for conical worm. The use of these methods makes it possible to explore the mistakes arising during production (e.g. thread pitch in axial plane, error of profile shape in axis or remarkable plane etc.) and to define the value of these errors.

2. Conical helical surfaces

In technical practice conical worm surfaces, which can be used in many ways, are most widely applied as a function surface of conical worms. The conical worm – crown wheel pairs spiroid drive, can be used for example as jointless drives of robots and tool machines [4].

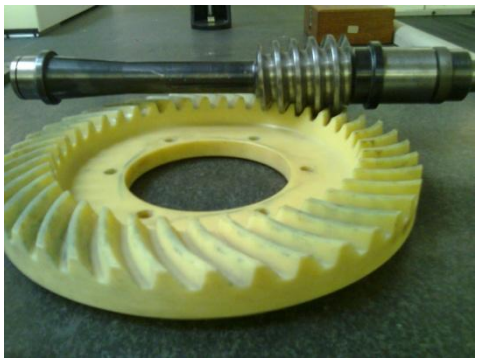

Figure 1: Spiroid worm gear drive

The jointless drives are attained by simply shifting (setting) the worm in an axial direction. The cog surface of the conical worm of the spiroid drives (Figure 1) can be attained the same way as that of the cylindrical worm, but besides the axial shift of the hob, a tangentional shift must be done depending on the conicity of the worm. Different – evolvent, Archimedean and convolute - helical surfaces can be defined in case of spiroid worm surface similar to the line surface cylindrical worm.

The dentation of crown wheel is produced with hob which tiler surface is similar to conical worm surface [4]. This is called direct motion mapping.

With these modern drive pairs, which are characterized by favourable hidrodinamic conditions, great strength and high efficiency, the energy loss in the gear can be reduced significantly. In power dissipation it is important to apply those cog geometrical

characteristics which result in good connection terms.

3. Manufacture of helicoidal surfaces in modern intelligent integrated system

At each stage in the process of production of worm gear drives, during design, manufacture and assembly, faults can occur. Modern intelligent integrated systems (ISS) can handle manufacturing in a versatile and flexible way; they can be efficiently utilized both in design and at the different phases of manufacture to improve product quality. Artificial intelligence and expert systems can now be used in the production of worm gear drives.

The intelligent integrated system (ISS) (for worm gear drives) provides the following:

1. Giving design specifications (module, number of threads, number of revolutions, etc.);
2. Detailed design (choice of engineering material, determination of basic geometric data, etc.);
3. Checking of documentation;
4. Preparing CAD drawings;
5. Manufacture;
6. Measurements.

During measurement the tasks are checking with CNC device the surface determined using basic data, analysis of the deviations and feeding them back into manufacturing process (eg wheel profile, machine and tool adjustments, etc.) [6].

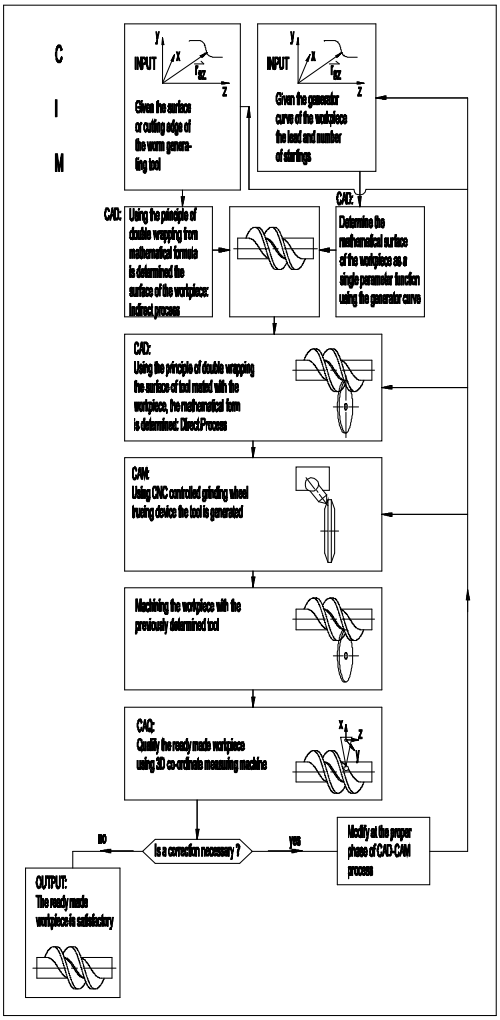

Figure 2: Production of helicoidal surfaces in CIM system [5]

4. The measuring machine

With the coordinate measuring machine (Figure 3) the surface points of the workpiece can be scanned with a touch unit starting from the orthographical machine coordinate system which is fixed in the measuring space defined by the leads of the measuring machine.

We measure the moving paths with a digital measuring system [2, 8]. The position of the touch unit along the coordinate axis is registered by a length measuring system and with these measurement results the surfaces of the workpiece can be defined by calculation.

The coordination measuring technique considers the workpieces to be a set of 2D and 3D surface elements replacing them with i=1,2,..,n measuring points in space.

The measuring machine puts compensator curves and surfaces on the measuring points by methods of analytic geometry and numerical analysis. This way we can define their parameters, the distance between them and their positions compared to each other. This principle can be used for measuring irregular workpieces.

Figure 3: DEA type 3 coordination measuring machine

We define the place of the workpiece by touching its surface points [1, 3]. In this case the most characteristic method is the Scanning technique for defining the measured surfaces. The main point of this technique is that the motion of the measure head is controlled into two coordinate directions only, the touch unit automatically stands into the third coordinate direction in a way to follow the shape of the surface. The machine records the coordinates of the middle point of the touch unit for defined deviation. We can only approximately define effective surface defined by the middle point of the touch unit.

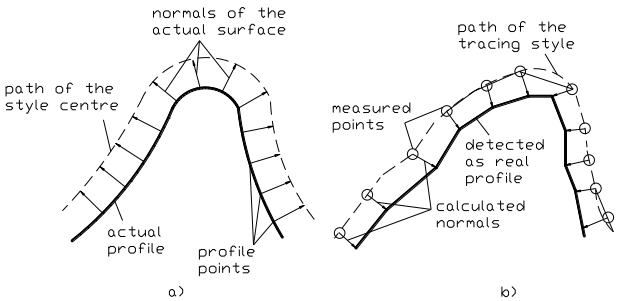

Figure 4: Defining the effective touching point

We can approximately define the effective surface points as the following:

- we define compensator curves or compensator surfaces on points which were defined by the touch unit;
- then the points of the effective surface could be defined from the surfaces to r touching distance along the normal vectors of a compensator surface.

This method is an approximate one because on the one hand the compensator surface has an approximate feature, on the other hand the effective touching point can be defined on the normal vector of this surface (Figure 4.b), however the middle point of the touch unit is on the normal vector of the real surface (Figure 4.a).

Integrating manufacturing system the measuring machine can be worked as a flexible manufacturing system in the factory (Figure 2).

5. Mathematical modelling of line forming conical helical surface

The r_g leading curve, a K_0 (ξ, η, ζ) is given in the tool coordinate system and its equation of the η coordinate function. That is:

$$\vec{r}_g = \vec{r}_g(\eta) \tag{1}$$

Since we consider the η coordinate an independent variable, the equation of the leading curve is:

$$\vec{r}_g = \xi(\eta)\cdot\vec{i} + \eta\cdot\vec{j} + \zeta(\eta)\cdot\vec{k} \tag{2}$$

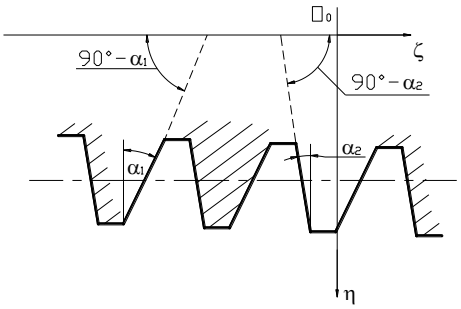

Figure 5: Determination of generator in axial section

The coordinates of an oblique point of the profile generator can be expressed as:

$$M_j\left[0, \eta, -\frac{\eta - b_1}{m_1}\right] \tag{3}$$

$$M_b\left[0, \eta, +\frac{\eta - b_2}{m_2}\right] \tag{4}$$

Carrying out a p_a axial and p_r radial helical motion of the K_0 (ξ, η, ζ) coordinate system – which includes the r_g leading curve – along the z axis and the y axis alternatively includes, the leading curve touches a conical helical surface in the K_{1F} (x_{1F}, y_{1F}, z_{1F}) an independent position and equals K_0 coordination system before the helical motion (Figure 6).

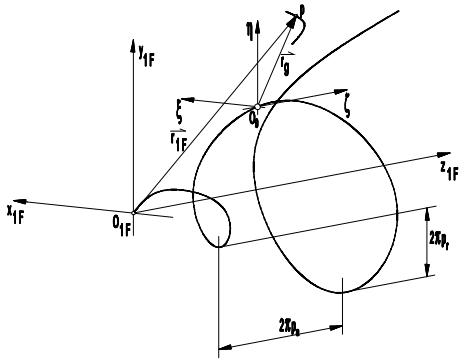

Figure 6: Touched thread surface by leading curve [4]

The helical surface touched by r_g curve in the K_{1F} (x_{1F}, y_{1F}, z_{1F}) coordinate system is:

$$\vec{r}_{1F} = M_{1F,0}\cdot\vec{r}_g \tag{5}$$

$$M_{1F,0} = \begin{bmatrix} \cos\vartheta & -\sin\vartheta & 0 & 0 \\ \sin\vartheta & \cos\vartheta & 0 & p_r\cdot\vartheta \\ 0 & 0 & 1 & p_a\cdot\vartheta \\ 0 & 0 & 0 & 1 \end{bmatrix} \tag{6}$$

We get the equations of the right (7) and left (8) profile sides by carrying out the (5) coordinate transformation operation:

$$\vec{r}_{1Fj} = \begin{bmatrix} -\eta\cdot\sin\vartheta \\ \eta\cdot\cos\vartheta + p_r\cdot\vartheta \\ -\frac{\eta - b_1}{m_1} + p_a\cdot\vartheta \\ 1 \end{bmatrix} \tag{7}$$

$$\vec{r}_{1Fb} = \begin{bmatrix} -\eta\cdot\sin\vartheta \\ \eta\cdot\cos\vartheta + p_r\cdot\vartheta \\ +\frac{\eta - b_2}{m_2} + p_a\cdot\vartheta \\ 1 \end{bmatrix} \tag{8}$$

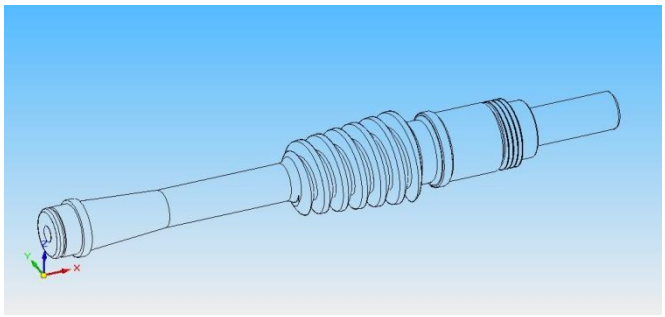

Figure 7: Mathematical model of conical helical surface

The conical surface is a function of η and ϑ :

$$\vec{r}_{1F} = \vec{r}_{1F}(\eta, \vartheta) \tag{9}$$

It is a well known fact that if a sphere and an optional surface touch each other, the normal vector in the touch point of the surface goes through the central point of the touching ball [6].

We use this regularity to define the contact point of the theoretical and substantial helical surfaces. For this we have to know the normal vector of the theoretical helical surface:

$$\vec{n} = \frac{\partial\vec{r}_{1F}}{\partial\eta}\times\frac{\partial\vec{r}_{1F}}{\partial\vartheta} = \begin{bmatrix} \vec{i} & \vec{j} & \vec{k} \\ \frac{\partial x_{1F}}{\partial\eta} & \frac{\partial y_{1F}}{\partial\eta} & \frac{\partial z_{1F}}{\partial\eta} \\ \frac{\partial x_{1F}}{\partial\vartheta} & \frac{\partial y_{1F}}{\partial\vartheta} & \frac{\partial z_{1F}}{\partial\vartheta} \end{bmatrix} \tag{10}$$

Solving the determinant the $\vec{n}$ vector can be defined by $\vec{i}, \vec{j}, \vec{k}$ unit vectors:

$$\vec{n} = \left(\frac{\partial y_{1F}}{\partial\eta}\cdot\frac{\partial z_{1F}}{\partial\vartheta} - \frac{\partial z_{1F}}{\partial\eta}\cdot\frac{\partial y_{1F}}{\partial\vartheta}\right)\cdot\vec{i} - \left(\frac{\partial x_{1F}}{\partial\eta}\cdot\frac{\partial z_{1F}}{\partial\vartheta} - \frac{\partial z_{1F}}{\partial\eta}\cdot\frac{\partial x_{1F}}{\partial\vartheta}\right)\cdot\vec{j} + \\ + \left(\frac{\partial x_{1F}}{\partial\eta}\cdot\frac{\partial y_{1F}}{\partial\vartheta} - \frac{\partial y_{1F}}{\partial\eta}\cdot\frac{\partial x_{1F}}{\partial\vartheta}\right)\cdot\vec{k} \tag{11}$$

Where:

$$n_{1Fx} = \frac{\partial y_{1F}}{\partial\eta}\cdot\frac{\partial z_{1F}}{\partial\vartheta} - \frac{\partial z_{1F}}{\partial\eta}\cdot\frac{\partial y_{1F}}{\partial\vartheta}$$

$$n_{1Fy} = -\frac{\partial x_{1F}}{\partial\eta}\cdot\frac{\partial z_{1F}}{\partial\vartheta} + \frac{\partial z_{1F}}{\partial\eta}\cdot\frac{\partial x_{1F}}{\partial\vartheta} \tag{12}$$

$$n_{1Fz} = \frac{\partial x_{1F}}{\partial\eta}\cdot\frac{\partial y_{1F}}{\partial\vartheta} - \frac{\partial y_{1F}}{\partial\eta}\cdot\frac{\partial x_{1F}}{\partial\vartheta}$$

So the normal vectors in case of right (13) and left (14) profile sides:

$$\vec{n}_j = \left(\cos\vartheta \cdot p_a - \frac{\eta \cdot \sin\vartheta + p_r}{m_1}\right)\cdot\vec{i} + \\ + \left(\sin\vartheta \cdot p_a + \frac{\eta \cdot \cos\vartheta}{m_1}\right)\cdot\vec{j} + (\eta - \sin\vartheta \cdot p_r)\cdot\vec{k} \quad (13)$$

$$\vec{n}_b = \left(\cos\vartheta \cdot p_a + \frac{\eta \cdot \sin\vartheta - p_r}{m_2}\right)\cdot\vec{i} + \\ + \left(\sin\vartheta \cdot p_a - \frac{\eta \cdot \cos\vartheta}{m_2}\right)\cdot\vec{j} + (\eta - \sin\vartheta \cdot p_r)\cdot\vec{k} \quad (14)$$

Knowing this fact, the normal vector goes through the $r_t(x_t, y_t, z_t)$ sphere centre point, the touching point of the theoretical helical surface can be defined. It is given by the $\vec{n}$ normal vector line going through $r_t(x_t, y_t, z_t)$ feeler centre and the thrust point of the theoretical helical surface, that is:

$$\left.\begin{aligned}\vec{n}(\vec{r}_t - \vec{r}_{1F}) = 0 \\ \vec{r}_{1F} = \vec{r}_{1F}(\eta, \vartheta)\end{aligned}\right\} \quad (15)$$

Where:

$$\vec{n}_j(\vec{r}_t - \vec{r}_{1Fj}) = \begin{bmatrix} n_{jx} & n_{jy} & n_{jz} & 1\end{bmatrix}\cdot\left(\begin{bmatrix} x_t \\ y_t \\ z_t \\ 1\end{bmatrix} - \begin{bmatrix} -\eta\cdot\sin\vartheta \\ \eta\cdot\cos\vartheta + p_r\cdot\vartheta \\ -\frac{\eta - b_1}{m_1} + p_a\cdot\vartheta \\ 1\end{bmatrix}\right) = 0 \quad (16)$$

$$\vec{n}_b(\vec{r}_t - \vec{r}_{1Fb}) = \begin{bmatrix} n_{bx} & n_{by} & n_{bz} & 1\end{bmatrix}\cdot\left(\begin{bmatrix} x_t \\ y_t \\ z_t \\ 1\end{bmatrix} - \begin{bmatrix} -\eta\cdot\sin\vartheta \\ \eta\cdot\cos\vartheta + p_r\cdot\vartheta \\ +\frac{\eta - b_1}{m_1} + p_a\cdot\vartheta \\ 1\end{bmatrix}\right) = 0 \quad (17)$$

That is:

$$\eta = \frac{\vartheta\cdot\left(p_r\cdot n_{jy} + p_a\cdot n_{jz}\right) - n_{jx}\cdot x_t - n_{jy}\cdot y_t - n_{jz}\cdot z_t + \frac{b_1}{m_1}\cdot n_{jz}}{n_{jx}\cdot\sin\vartheta - n_{jy}\cdot\cos\vartheta + \frac{n_{jz}}{m_1}} \quad (18)$$

$$\eta = \frac{\vartheta\cdot\left(p_r\cdot n_{by} + p_a\cdot n_{bz}\right) - n_{bx}\cdot x_t - n_{by}\cdot y_t - n_{bz}\cdot z_t - \frac{b_1}{m_1}\cdot n_{bz}}{n_{bx}\cdot\sin\vartheta - n_{by}\cdot\cos\vartheta - \frac{n_{bz}}{m_1}} \quad (19)$$

During solution the ϑ parameter is stepped and we define the η values for every ϑ value.

Putting the received η and ϑ parameters in (9) we get the x_{1F}, y_{1F}, z_{1F} coordinates of the touching point of the theoretical thread surface.

The real touch point is situated on the surface of the sphere touch unit, that is it can be found r distance from the central point of the touch unit. This normal direction distance means Δx, Δy, Δz projection distance in the different coordinate directions.

The Δx, Δy, Δz receive different values depending on the position of the touching point:

$$\Delta x = \frac{n_x}{|n|}\cdot r \\ \Delta y = \frac{n_y}{|n|}\cdot r \quad (18) \\ \Delta z = \frac{n_z}{|n|}\cdot r$$

According to these we can define the actual touch points (with HELICAM software) and we can calculate the divergences from the theoretical points.

6. Carrying out the measurement

We carried out the measurement on a spiroid worm (Figure 7) [7]. On the basis of the measured results (conicity, thread pitch, profile shape) and the theoretical knowledge we define differences and conclude the quality of the worm.

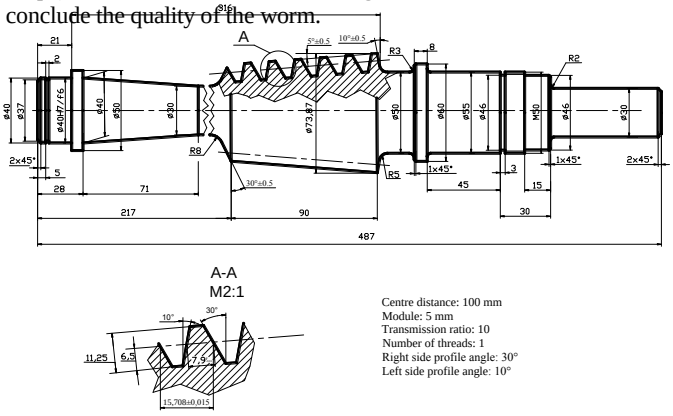

Figure 8: Technical drawing of our examed spiroid worm

6.1. The adoption of the coordination system of the worm

We fix the worm into a prism for the measuring (Figure 9).

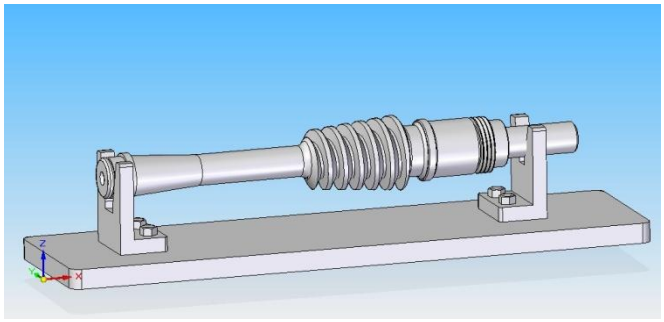

Figure 9: Fix the worm into a prism for the measuring

We put 3 points on the desk of the coordinate machine for the coordinate system of the worm. We put a plane on the three points with PC–DMIS measuring software which we move to the axis plane of the worm. We put 3 points on the right and 3 points on the left side of the worm. These are points 1, 2, 3 on Figure 10. Based on the adopted points we draw circles and the connecting line of the middle points of the two circles will be the worm axis, which is X axis. We get Z coordinate axis if we put a random point on the worm and the perpendicular line gives Z axis from the random point to X axis. The Y direction is a perpendicular direction on the received X and Z coordinate directions (Figure 10).

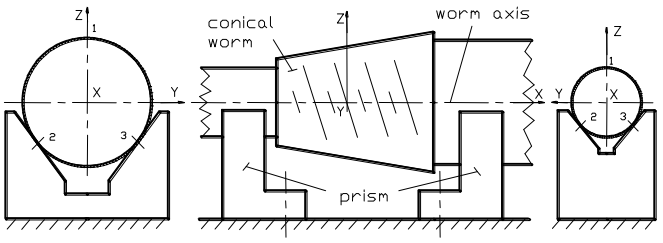

Figure 10: The adoption of the coordination system of the worm

6.2. Measuring conicity

Each head ribbon surface in the worm has to be touched by the touch unit, the y values is fixed. The plotted points are situated

theoretically on one line (Figure 11).

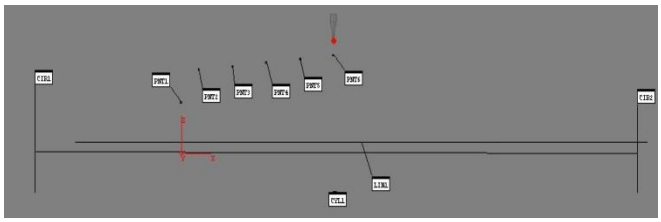

Figure 11: The plotted points of the head ribbon

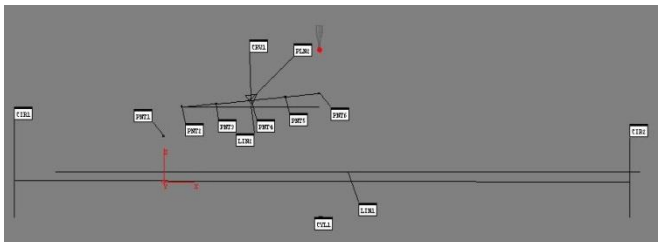

Figure 12: Placing regression line on the measured points

We put a regression line on the measured points (PNT2-PNT6) with the software that is why we define the angle between the regression line and the theoretical middle line of the worm (Figure 12). The effective angle value is the double of the received half angle (α). Comparing the effective angle with the nominal angle (10°±10') we get the dimension of the error. Measured angle: 9º 55'.

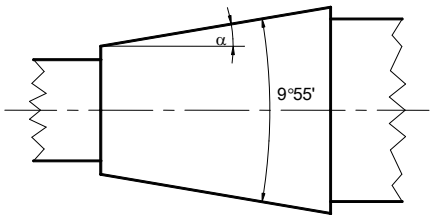

Figure 13: The measured conical angle and the α half angle

Based on these we can determine that, the measured conical angle is in the tolerance level. On Figures 11 and 12 the PNT1 point is the point which has to be adopted for Z axis.

6.3. Profil shape measuring

The error of the worm profile is such a perpendicular distance between two theoretical correct shape cog profile which surrounds the real cog profile inside the working profile section (f_r). Figure 14 demonstrates the theoretical basis of the examination.

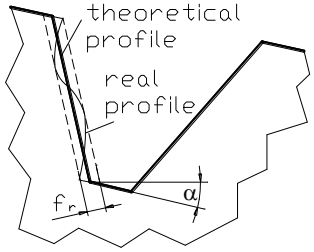

Figure 14: Definition of the error of the worm profile shape

We have to carry out the measuring of the error of the worm profile shape in the main plane of the worm in the plane of the nominal profile. We have to define the differences of the theoretical profile from the real profile and represent their differences the value of the profile shape could be defined. It means different h_1, h_2, … , h_n differences. We can define the value of the middle differences with averaging of these differences:

$$h_{mid} = \frac{h_1 + h_2 + \ldots + h_n}{n} \tag{19}$$

The sum of the absolute value of the minimum and maximum differences gives the value of the error of the profile:

$$f_r = \left|\Delta^+_{h\max}\right| + \left|\Delta^-_{h\max}\right| \tag{20}$$

The received f_r error value has to be smaller than the tolerance of the f_r profile error (MSZ 05.5502-75).
Carrying out the measurement:

1) Choose the surface scanning menu point in the PC-DMIS program.
2) Give these parameters:
   - the starting point of the scanning (give the first point by touching),
   - the direction of the surface scanning (creating the direction vector from the starting point and from the next point in the given direction),
   - the end point of the scanning (giving the final point by touching).
3) After completing the measurement we similarly have the scanning technology done for four other cog profiles.
4) We compare the measured profiles with the theoretical profile.

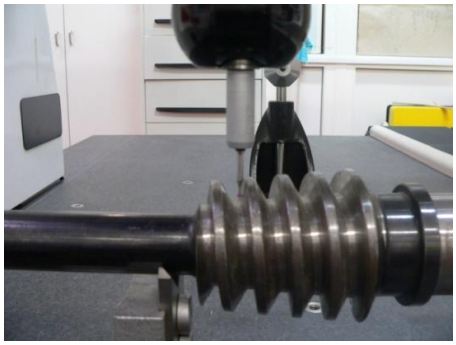

Figure 15: Surface scanning

x	y	z		x	y	z
1.088	21.469	4.805		1.314	29.872	44.547
1.092	23.99	5.249		1.318	27.669	45.824
1.093	26.486	5.695		1.329	25.419	47.125
1.091	28.976	6.154		1.334	23.857	48.163
1.092	30.803	6.466		1.347	26.503	52.04
1.094	31.193	7.016		1.353	28.487	52.407
1.112	31.409	9.266		1.355	30.456	52.769
1.124	30.559	11.174		1.354	32.94	53.233
1.14	27.924	12.702		1.356	34.811	53.531
1.149	25.735	13.976		1.361	35.149	53.956
1.156	23.57	15.258		1.373	35.391	55.671
1.16	22.228	15.991		1.382	35.534	57.161
1.161	22.696	20.47		1.397	33.735	58.786
1.17	27.452	21.325		1.398	31.981	59.805
1.17	29.943	21.781		1.41	30.25	60.809
1.172	31.955	22.057		1.415	28.089	62.065
1.176	32.435	22.481		1.444	27.96	67.753
1.195	32.752	24.974		1.442	29.916	68.116
1.209	31.981	26.839		1.444	31.889	68.482
1.219	29.265	28.414		1.441	34.36	68.944
1.224	27.068	29.688		1.443	36.208	69.276
1.236	24.918	30.929		1.443	36.532	69.72
1.259	26.444	36.585		1.457	36.752	71.474
1.261	28.405	36.948		1.468	36.802	73.164
1.261	30.382	37.31		1.482	34.966	74.557
1.267	32.8	37.756		1.484	33.244	75.558
1.272	33.923	38.546		1.498	31.514	76.565
1.292	34.14	41.027		1.506	29.314	77.837
1.298	33.659	42.342		1.514	27.642	78.802
1.306	31.599	43.552				

Figure 16: The received profile points by surface scanning (in axial

plane)

We saved the received points usable format for CAD systems with PC-DMIS software (Figure 17), then we prepared the real worm based on the received points. We prepared the theoretical worm with CAD software. We assembled the theoretical and the real worm and defined the value of the profile shape mistake.

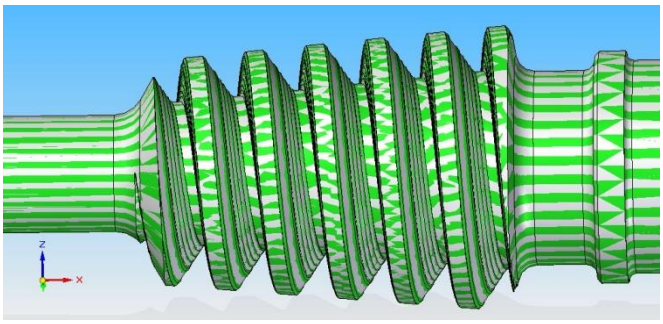

Figure 17: Comparison of the theoretical (grey color) and the real (green color) worm

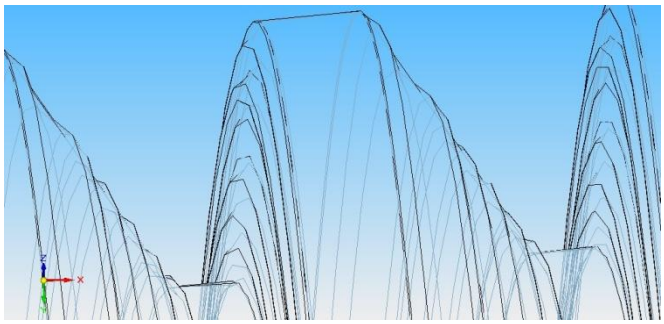

Figure 18: Evaluation of profile shape error

We worked out the mathematical evaluation too. We put the received points with surface scanning and the theoretical profile points to the equations of the spiroid worm (7), (8). Based on the differences of the appropriate point pairs and the sum of absolute value of the maximum (positive) and minimum (negative) differences give the value of the profile shape error.

Based on the modelling and calculation we determined the difference of the real profile of the examined spiroid worm from the theoretical profile is in the tolerance level (IT 6).

6.4. Thread pitch measuring

We do the scanning for two neighbouring cog profiles in axial section like we did when we measured the profile shape deviation (Figure 19).

We have to put a geometrical element on the profiles by means of which we can clearly define the distance of the two profiles. This geometrical element is the line. We define the axial direction distance of the two lines. This value will be the thread pitch.

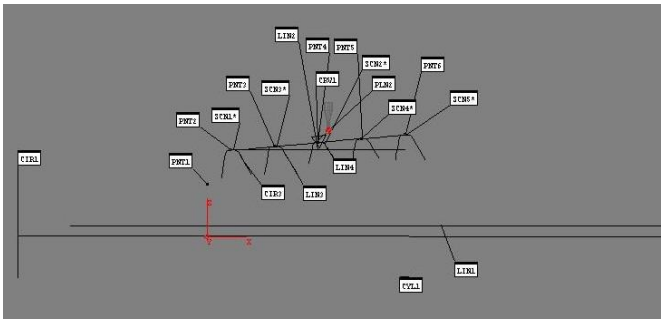

Figure 19: Thread pitch measuring

Measured thread pitch: 15,717 mm
Prescribed thread pitch: 15,708±0,015 mm

The measured thread pitch is inside the tolerance level of the prescribed drawing thread pitch (Figure 8). So the thread pitch of the worm is appropriate.

7. Summary

We have developed an up–to-date measuring method, the measuring of thread surfaces without circle desk for conical worm.

We defined the equation of the line forming spiroid worm in case of right and left profile side using matrix geometric method, then defined the equations of the normal vectors.

We carried out the analysis of measuring technique of conicity, error of the profile shape and thread pitch of the line forming spiroid worm. Based on the received measuring results and the prescribed geometric values we defined the characteristics of the spiroid worm is in the tolerance level so the spiroid worm is appropriate. This method is appropriate for helical surface classification.

Integrating manufacturing system the measuring machine can be worked as a flexible manufacturing system in the factory.

ACKNOWLEDGEMENT

This work was supported by OTKA project K 63377. entitled ”Complex analysis of the features of production geometry and meshing in case of up-to-date application” (2006-2010).
Research leader: Dr. Illés Dudás, DSc Professor.

REFERENCES

1. Bányai Károly: Hengeres csigák gyártás- geometriája és ellenőrzése, Egyetemi doktori disszertáció, kézirat 1987.
2. Bodzás Sándor - Pudmer Sándor: Csiga és Csigakerék mérése 3 koordinátás mérőgéppel, TDK dolgozat, Miskolci Egyetem, 2008.12.04.
3. Bodzás Sándor: „OL-3-as lemezolló csigakerék” gyártásának minőségbiztosítása, Diplomamunka, Miskolci Egyetem, 2009, 2009 - GGT39
4. Dr. Dudás Illés: The Theory and Practice of Worm Gear Drives. Penton Press, London, 2000. (ISBN 1 8571 8027 5)
5. Dr. Dudás Illés: Csigahajtások elmélete és gyártása, Budapest, Műszaki könyvkiadó, 2007. (ISBN 978 963 16 6047 0)
6. Dr. Dudás Illés – Dr. Bányai Károly – Bajáky, Zs.: Koordináta méréstechnika alkalmazása a csavarfelületek minősítésére, VIII. Nemzetközi Szerszámkonferencia Miskolc, 1993.
7. Hegyháti, J: Untersuchungen zur Anwendung von Spiroidgetrieben. Diss. A. TU. Dresden, 1988. p. 121.
8. Hörcsik Renáta: 3D measurement with two different software, microCAD 2005 Proceedings of International Scientific Conference, Section M1: Production Engineering and Manufacturing Systems, March 10-11. 2005., University of Miskolc, Hungary